DOI: 10.1002/anie.200805415

Prussian Blue Analogues

Revisiting Prussian Blue Analogues with Solid-State MAS NMR Spectroscopy: Spin Density and Local Structure in $[Cd_3\{Fe(CN)_6\}_2]\cdot 15H_2O$**

*Alexandrine Flambard, Frank H. Köhler, and Rodrigue Lescouëzec**

Prussian blue analogues (PBAs) are three-dimensional inorganic solids whose apparently simple composition (cyanide ligands connecting metal ions) and structure (cubic) cover a large family of (often nonstoichiometric) compounds. Beyond the general formula $[A_nM'_x\{M(CN)_6\}_y]\cdot z\,H_2O$ (M,M′ = transition metal ions, A = optional alkali-metal ion), the infinite variation of composition leads to a wide variety of physical behaviors and potential technological applications.[1] For instance, the porous character of PBAs makes them candidates for waste recovery,[2] hydrogen storage,[3] and heterogeneous catalysis.[4] Molecular magnetism is a recent topic in which the hexacyanometallate precursors $[M(CN)_6]^{x-}$ have proven successful, because the ambidentate cyanide ligand is suitable for the assembly of heterometallic compounds and has a remarkable ability to transmit an effective magnetic exchange interaction. The tuning of the Curie temperature,[5] Fe–Co photoinduced[6] or Cr–Cr electroinduced[7] switchable magnetism, and Fe–Mn multiferroic behavior[8] are striking results achieved with magnetic PBAs. In these compounds, the structural parameters, such as the number of vacancies, the alkali-metal-ion content, and the M′-N-C angle, play an important role in the physical properties of the material.

X-ray diffraction is the technique of choice for structural characterization of these highly insoluble coordination polymers. However, most of the powder studies afford only general data of the lattice, while single crystals are difficult to obtain and lead to an average structure. By applying techniques such as extended X-ray absorption fine structure (EXAFS)[9] and Mössbauer spectroscopy,[10] precious local structural information has been gained, leading to better insight into the physical properties. Nevertheless, these two techniques either require elaborate instrumental setup or are limited to iron in routine studies. These limitations may be overcome by NMR spectroscopy, which has become a common technique in modern laboratories, even for paramagnetic compounds.[11] Herein, magic-angle spinning (MAS) solid-state NMR spectroscopy has been chosen as a novel approach complementary to X-ray diffraction for the study of magnetic PBAs. On the one hand, the NMR spectroscopic response can be used as a local probe to extract structural information, as the chemical shift of the observed nucleus is very dependent on its environment. On the other hand, paramagnetic NMR spectroscopy studies give insight into how spin density extends from the paramagnetic source toward the periphery. Indeed, the chemical shift depends on the hyperfine coupling (the interaction between the unpaired electron and the observed nucleus), which is related to the amount of spin density on the nucleus. Overall, MAS NMR spectroscopy can help us deduce the local metal coordination and the spin-transfer mechanism, both of which affect the magnetic properties.

Preliminary studies on hexacyanometallate building blocks have shed light on the mechanism of spin transfer onto the cyanide ligand by accurately measuring the spin density on the carbon and nitrogen atoms.[12] However, related studies on how spin extends over the cyanide bridge onto the second metal center M′ in the resulting PBAs has never been reported. Herein, we present a MAS NMR spectroscopy study on a series of mixed PBAs of formula $[Cd^{II}_3\{Fe^{III}_xCo^{III}_{1-x}(CN)_6\}_2]\cdot 15H_2O$ with $x = 0$ (**1**), 0.25 (**2**), 0.5 (**3**), 0.75 (**4**), and 1 (**5**). Cadmium has been selected as a diamagnetic probe because the ^{113}Cd isotope has a $^1/_2$ nuclear spin and sufficient receptivity. By using low-spin Fe^{III} ($S = {}^1/_2$) as a paramagnetic source, we have been able to determine for the first time the spin-transfer mechanism at work in these PBAs. More importantly, an alternative picture to the well-known structural model of PBAs based on common X-ray diffraction techniques has been established.

A dozen single crystal X-ray analyses have been reported for $[M^{II}_3\{M^{III}(CN)_6\}_2]\cdot x\,H_2O$ compounds,[13] including the diamagnetic compound $[Cd^{II}_3\{Co^{III}(CN)_6\}_2]\cdot 15H_2O$ (**1**)[14] and the paramagnetic sample $[Cd^{II}_3\{Fe^{III}(CN)_6\}_2]\cdot 15H_2O$ (**5**).[15] Their structure can be described as a cubic lattice in which alternating octahedral divalent and trivalent metal centers are linked through cyanide edges along the three crystallographic axes (Figure 1). According to their stoichiometry, only two thirds of the $\{M^{III}(CN)_6\}$ sites are occupied, leaving one third vacancies (□). Each vacancy contains six water molecules coordinated to six nearest M^{II} ions and a variable amount of crystallization water. The unit cell can

[*] Dr. A. Flambard, Dr. R. Lescouëzec
Institut Parisien de Chimie Moléculaire
Université Pierre et Marie Curie-Paris6, UMR 7071
Paris 75252 (France)
E-mail: rodrigue.lescouezec@upmc.fr
Prof. Dr. F. H. Köhler
Technische Universitat München
Lichtenbergstrasse 4, 85747 Garching (Germany)

[**] This work was supported by the Centre National de la Recherche Française (CNRS, France), the Ministère de l'Enseignement Supérieur et de la Recherche (MESR, France), and the Bayerisch–Französisches Hochschulzentrum. The technical assistance of Dr. E. Pardo, Dr. G. Raudaschl-Sieber, and B. Revel is gratefully acknowledged. MAS = magic-angle spinning.

Supporting information for this article is available on the WWW under http://dx.doi.org/10.1002/anie.200805415.

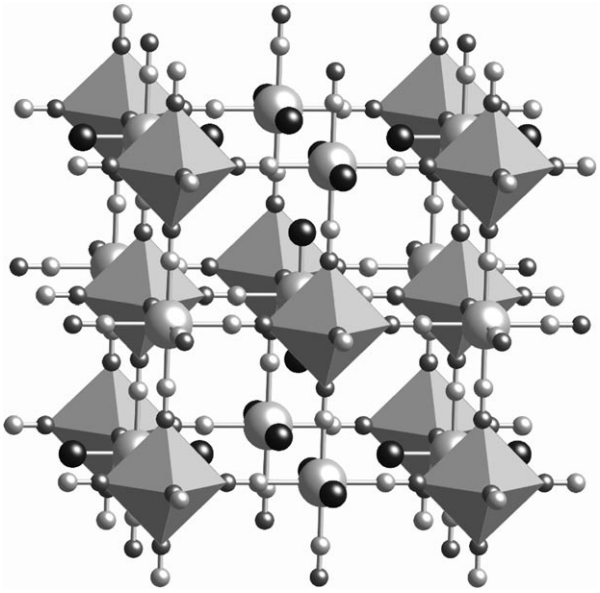

Figure 1. Idealized cubic structure of $[Cd_3\{M(CN)_6\}_2]\cdot x\,H_2O$ (interstitial water omitted). Octahedra: $(Fe/Co)C_6$ moities; large light gray spheres: Cd^{II} ions; small black spheres: coordinated H_2O; small dark gray spheres: C; small light gray spheres: N.

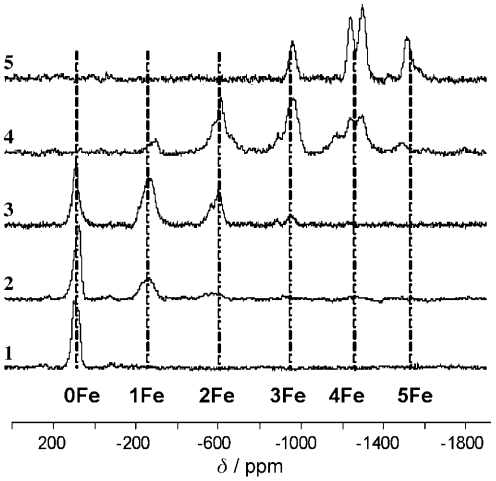

Figure 2. ^{113}Cd MAS NMR spectra of $[Cd_3\{Fe_xCo_{1-x}(CN)_6\}]\cdot 15\,H_2O$. Iron contents are $x = 0$ (**1**), 0.25 (**2**), 0.5 (**3**), 0.75 (**4**), and 1 (**5**). Dotted lines refer to six different cadmium surroundings having a variable number of neighboring iron ions. The spectra were recorded at 310 K at a MAS frequency of 10 kHz.

thus be formulated as $[M^{II}_4\{M^{III}(CN)_6\}_{8/3}\square_{4/3}]\cdot x\,H_2O$ ($x = 12$–20), and the average M^{II} coordination sphere is $M^{II}(NC)_4(OH_2)_2$. From this general description of the structure derived from X-ray and elemental analyses, two different microscopic views can be proposed: 1) Vacancies are ordered in the solid such that only divalent sites with neutral charge $Cd^{II}(NCFe)_4(OH_2\square)_2$ are present. 2) Vacancies are randomly distributed so that up to seven different M^{II} environments $Cd^{II}(NCFe)_{6-x}(OH_2\square)_x$ with $x = 0$–6) are present.[16] NMR spectroscopy has been used to gain a better view of the local structure of PBAs.

The ^{113}Cd MAS NMR spectrum of the diamagnetic cobalt compound $[Cd^{II}_3\{Co^{III}(CN)_6\}_2]\cdot 15\,H_2O$ (**1**, Figure 2) exhibits two overlapping signals at $\delta = +63$ and $+81$ ppm in the expected diamagnetic range ($\delta = +500$ to -125 ppm).[17] At first glance, this result could be attributed to a $Cd(NCCo)_4(OH_2)_2$ site exhibiting isomeric environments with either two *cis* or two *trans* water molecules. This situation would agree with an ordered distribution of vacancies in the solid. As expected, the spectrum of the paramagnetic iron derivative $[Cd^{II}_3\{Fe^{III}(CN)_6\}_2]\cdot 15\,H_2O$ (**5**, Figure 2) is strongly affected by the hyperfine interaction. It shows four main ^{113}Cd peaks strongly shifted out of the diamagnetic range, which correspond to four distinct cadmium sites. Interestingly, these observations do not match with an ordered distribution of the vacancies in the lattice, for which one peak would be expected, as for the Co^{III} sample. The central pair of signals at $\delta = -1275$ and -1327 ppm could be attributed to isomeric cadmium environments $Cd(CNFe)_4(OH_2)_2$, as suggested for the diamagnetic sample. The additional peaks, appearing equidistant on both sides of the central resonance at $\delta = -1000$ and -1537 ppm, are necessarily due to cadmium ions lying in very different environments. As the amount of unpaired electron density (or electron spin density) on the observed nucleus has a major influence on the chemical shift, we may assume that cadmium ions surrounded by either three or five paramagnetic iron ions are responsible for these two additional resonances. The more iron ions in the environment of the cadmium center, the more spin density is delocalized on the cadmium nucleus and the more shifted are the signals. The resonance at $\delta = -1000$ ppm may thus be assigned to a $Cd(CNFe)_3(OH_2)_3$ site, whereas the resonance at $\delta = -1537$ ppm may be attributed to a $Cd(CNFe)_5(OH_2)$ site.

To confirm these assumptions, mixed iron/cobalt PBAs $[Cd_3\{Fe/Co(CN)_6\}_2]\cdot 15\,H_2O$ (**2**–**4**) were synthesized so that an overall series with iron content of 0 (**1**), 25 (**2**), 50 (**3**), 75 (**4**), and 100 % (**5**) was available.[18] The ^{113}Cd MAS NMR spectra (Figure 2, traces **1**–**5**) exhibit a total of six signal ranges separated from each other by $\delta = 300$–350 ppm. The relative signal intensities depend on the Fe/Co ratio, but the shift ranges do not change. It follows that there are six types of cadmium sites in the samples. Their individual abundances and chemical shifts depend on the percentage of paramagnetic iron(III) ions in the sample and the number of adjacent iron ions per cadmium ion. The six signals can thus be assigned to the local coordination spheres described by $Cd(para)_y(dia)_{6-y}$ with $5 \le y \le 0$, where para and dia stand for paramagnetic (NCFe) and diamagnetic (NCCo or $OH_2\square$) ligand sites, respectively. We note, however, that $y = 6$ is not observed.

If vacancies were randomly distributed in the samples, seven signals should be observed, and peaks corresponding to $Cd(CNFe)_2(OH_2)$ and $Cd(CNFe)_6$ should be seen in **5**.[16] As they are not, it is clear that there is some restriction to a random distribution of vacancies. This restriction is explained by taking into account the local charge distribution. The average coordination $Cd(NCFe)_4(OH_2\square)_2$ (see above) has neutral balanced charge. When (NCFe) is replaced stepwise by vacancies ($OH_2\square$) and vice versa, cadmium sites $Cd(NCFe)_{4-y}(OH_2\square)_{2+y}$ exhibit a charge equal to $0.5\,y$ (with $-2 \le y \le 2$). For compound **5**, this situation would lead to local charges of up to ± 1 and to five ^{113}Cd signals in the NMR

spectrum. Hence, a charge imbalance of ± 1 has a low probability and only ± 0.5 can be observed. In this case, $-1 \leq y \leq 1$, and three ^{113}Cd signals for the moieties $\{Cd(NCFe)_3(OH_2\square)_3\}^{0.5+}$, $\{Cd(NCFe)_4(OH_2\square)_2\}^{0}$, and $\{Cd(NCFe)_5(OH_2\square)\}^{0.5-}$ with increasing shift to low frequency are observed.

Interestingly, additional peaks are resolved within the six cadmium signal shift areas. This finding may be ascribed to the *cis*/*trans* and *mer*/*fac* isomeric coordination spheres of $Cd(para)_4(dia)_2$, $Cd(para)_3(dia)_3$, and $Cd(para)_2(dia)_4$ centers. Finally, the assignment of the signal shift areas in Figure 2 has been further confirmed by variable-temperature studies (Figure 3). In fact, increasing the temperature does not affect the peaks near $\delta = 70$ ppm, as expected for the moiety $Cd(NCCo)_4(OH_2\square)_2$. In contrast, the chemical shifts of all other signal patterns decrease with increasing the temperature, which indicates the presence of spin in the coordination sphere of the Cd^{2+} ions. The chemical shift variation is more pronounced as the number of $\{Fe(CN)_6\}^{3-}$ units (and thus the amount of spin density) next to Cd^{2+} increases.

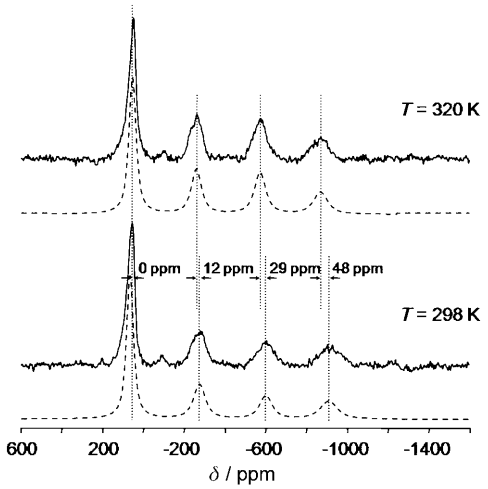

Figure 3. Temperature dependence of the ^{113}Cd spectrum (external temperature: 298 and 320 K) of **3**. Experimental and calculated spectra are shown by solid and dashed lines, respectively. The spectra were acquired at 7.1 T at a MAS frequency of 10 kHz.

At this point it is worthwhile to underline the complementarity of NMR spectroscopy and other techniques. The structural model deduced from elemental and X-ray analyses may lead to a wrong perception of the actual local structure, because divalent sites such as $M^{II}(NC)_3(OH_2)_3$ and $M^{II}(CN)_5(OH_2)$ cannot be identified, although they represent 40% of the total divalent sites according to the present MAS NMR spectroscopic analysis. The accurate qualitative and quantitative information available from NMR spectroscopy is due to the paramagnetic character of the samples. This relationship becomes obvious when the spectrum of **5** is compared with that of its diamagnetic analogue **1**, in which all cadmium sites overlap. Thus, a small but significant amount of spin density induces an enlargement of the spectral window, producing a magnifying-glass effect. Consequently, unlike techniques such as EXAFS or Mössbauer spectroscopy, MAS NMR spectroscopy discriminates between the different cadmium sites, and it is even the basis of quantitative approaches.

An example is precise information on the spin density, which is highly relevant to the magnetic ordering in PBAs. The spin density has been derived from the paramagnetic chemical shift. Remarkably, all shifts of ^{113}Cd signals in the NMR spectra of iron-containing samples are negative, which indicates a negative spin on the Cd^{2+} centers. In fact, the shifts are related to the spin density $\rho(N)$ through Equation (1),[19]

$$\rho(N) = \frac{9\,k\,T\,a_0^3}{\mu_0\,g_{av}^2\beta_e^2 S(S+1)}\,\delta_T^{con}(N) \qquad (1)$$

where k is the Boltzmann constant, μ_0 is the vacuum permeability, g_{av} is the mean electron g factor, β_e is the Bohr magneton, a_0 is the Bohr radius, S is the electron spin quantum number, and δ_T^{con} is the contact shift at the measuring temperature T. The average calculated spin densities on cadmium ions for the iron-containing samples **2**–**5** are -0.0027, -0.0054, -0.0088, -0.0106, and -0.0124 a.u. (see the Supporting Information). According to previous studies, the spin density on the C and N atoms of $\{Fe(CN)_6\}^{3-}$ is negative and positive, respectively.[12] Combining all data gives a complete map of spin densities on the $\cdots M^{III}$-C-N-M^{II}-N-C-$M^{III}\cdots$ backbone of $[Cd_3\{Fe(CN)_6\}_2]\cdot 15\,H_2O$ (Figure 4). The result is a pattern of spin signs that alternate when progressing from one atom to the next throughout the lattice. This situation accounts for the strong role of the spin polarization mechanism[19] in the spin transfer all the way from iron to cadmium. The presence of small but significant spin density at a remote position from the paramagnetic source could lead to a weak magnetic interaction between the iron atoms. Magnetic measurements of **2**–**5** down to 2 K (Figure SI2 in the Supporting Information) give $\chi_m T$ vs. T curves that are identical after scaling (taking into account the Co^{III} doping). This fact indicates that the magnetic interaction across the Cd^{2+} ions in $[Cd_3\{Fe(CN)_6\}_2]\cdot 15\,H_2O$ cannot be detected by measurement of the bulk. Once again, this result

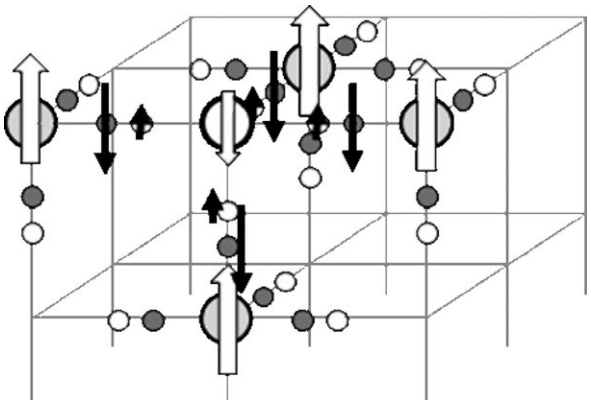

Figure 4. Spin sign pattern of $[Cd_3\{Fe(CN)_6\}_2]\cdot 15\,H_2O$. For clarity, one Cd^{2+} ion and its adjacent $\{Fe(CN)_6\}^{3-}$ ions are selected; large circles are Cd (white) and Fe (light gray), small circles are N (white) and C (dark gray). The arrows represent positive (up) and negative (down) spin densities. They represent the relative amount of spin but are not drawn to scale.

underlines the high sensitivity of NMR spectroscopy toward spin density detection.

In conclusion, MAS NMR spectroscopy studies performed herein give a clear-cut picture of the spin transfer and the local structure of PBAs. The presence of paramagnetic sources surrounding the observed nucleus has a magnifying-glass effect on the NMR spectrum and leads to a clear distinction and the quantification of the different divalent sites. Indeed, the actual structure differs significantly from the average view proposed by X-ray diffraction experiments. It has been shown that the distribution of vacancies in the lattice of PBAs is not fully random and can be quantified. Furthermore, local resolution of the geometric structure and the spin structure down to isomeric coordination spheres has been obtained. Such information is important, as physical properties of PBAs closely depend on their (local) structure. Hence this work shows promise for further studies such as spin mapping of other Prussian blue analogues as well as monitoring the incorporation of molecules and ions into the voids of dehydrated samples.

Experimental Section

$[Cd_3\{M(CN)_6\}]\cdot 15H_2O$ (M = Fe, Co): The compounds precipitated when an aqueous solution of $K_3[M(CN)_6]$ (3 mmol, 40 mL) was added dropwise to aqueous $CdCl_2$ (15 mmol, 10 mL). The obtained precipitate was washed three times with distilled water and dried in air (yield: 95%). Elemental analysis, metal content, characteristic IR spectroscopy bands, and XRD powder patterns are given in the Supporting Information.

XRD powder patterns were obtained with a Siemens D500 diffractometer back monochromatized using $Cu_{K\alpha}$ radiation. The NMR spectra were recorded on a Bruker AV300 spectrometer. The isotropic signal shifts δ_T^{para} at the measuring temperature T were determined relative to external adamantane and $Cd(NO_3)_2$ salt (see the Supporting Information).

Received: November 5, 2008
Published online: January 23, 2009

Keywords: NMR spectroscopy · Prussian blue analogues · solid-state structures · spin density

[1] a) B. Mij (Shell Int. Research), Pat Appl 84/00796, **1984**; b) E. Reguera, J. Fernandez, J. Duque, *Polyhedron* **1994**, *13*, 479–484; c) A. A. Karyakin, *Electroanalysis* **2001**, *13*, 813–819; d) R. Koncki, *Crit. Rev. Anal. Chem.* **2002**, *32*, 79–96; e) N. R. de Tacconi, K. Rajeshwar, R. O. Lezna, *Chem. Mater.* **2003**, *15*, 3046–3062; f) M. Verdaguer, G. S. Girolami, *Magnetism: Molecules to Materials V* (Eds.: J. S. Miller, M. Drillon), Wiley-VCH, Weinheim, **2005**, pp. 283–346.

[2] M. T. G. Valentini, R. Stella, L. Maggi, G. Ciceri, *J. Radioanal. Nucl. Chem.* **1987**, *114*, 105–111.

[3] S. S. Kaye, J. R. Long, *J. Am. Chem. Soc.* **2005**, *127*, 6506–6507.

[4] a) A. Karyakin, E. Karyakina, L. Gorton, *Anal. Chem.* **2000**, *72*, 1720–1723; b) A. S. Kumar, J. M. Zen, *ChemPhysChem* **2004**, *5*, 1227–1231.

[5] a) M. Verdaguer, A. Bleuzen, V. Marvaud, J. Vaissermann, M. Seuleiman, C. Desplanches, A. Scuiller, C. Train, R. Garde, G. Gelly, C. Lomenech, I. Rosenman, P. Veillet, C. Cartier dit Moulin, F. Villain, *Coord. Chem. Rev.* **1999**, *190*, 1023–1047; b) S. Ferlay, T. Mallah, R. Ouahès, P. Veillet, M. Verdaguer, *Nature* **1995**, *378*, 701–703; c) S. M. Holmes, G. S. Girolami, *J. Am. Chem. Soc.* **1999**, *121*, 5593–5594.

[6] a) O Sato, T. Iyoda, A. Fujishima, K. Hashimoto, *Science* **1996**, *272*, 704–705; b) V. Escax, A. Bleuzen, C. Cartier dit Moulin, F. Villain, A. Goujon, F. Varret, M. Verdaguer, *J. Am. Chem. Soc.* **2001**, *123*, 12536–12543.

[7] O Sato, T. Iyoda, A. Fujishima, K. Hashimoto, *Science* **1996**, *271*, 49–51.

[8] S. Ohkoshi, H. Tokoro, T. Matsuda, H. Takahashi, H. Irie, K. Hashimoto, *Angew. Chem.* **2007**, *119*, 3302–3305; *Angew. Chem. Int. Ed.* **2007**, *46*, 3238–3241.

[9] Recent example: A. Bleuzen, V. Escax, A. Ferrier, F. Villain, M. Verdaguer, P. Münsch, J.-P. Itié, *Angew. Chem.* **2004**, *116*, 3814–3817; *Angew. Chem. Int. Ed.* **2004**, *43*, 3728–3731.

[10] Recent examples : a) E. J. M. Vertelman, E. Maccallini, D. Gournis, P. Rudolf, T. Bakas, J. Luzon, R. Broer, A. Pugzlys, T. T. A. Lummen, P. H. M. van Loosdrecht, P. J. van Koningsbruggen, *Chem. Mater.* **2006**, *18*, 1951–1963; b) S. Gawali-Salunke, F. Varret, I. Maurin, C. Enachescu, A. Malarova, K. Boukheddaden, E. Codjovi, H. Tokoro, S. Ohkoshi, K. Hashimoto, *J. Phys. Chem. B* **2005**, *109*, 8251–8256.

[11] a) M. A. Shaibat, L. B. Casabianca, N. P. Wickramasinghe, S. Guggenheim, A. C. de Dios, Y. Ishii, *J. Am. Chem. Soc.* **2007**, *129*, 10968–10969; b) S. Balayssac, I. Bertini, M. Lelli, C. Luchinat, M. Maletta, *J. Am. Chem. Soc.* **2007**, *129*, 2218–2219; c) T. Jovanovic, A. McDermott, *J. Am. Chem. Soc.* **2005**, *127*, 13816–13821; d) G. Kervern, G. Pintacuda, Y. Zhang, E. Oldfield, C. Roukoss, E. Kuntz, E. Herdtweck, J.-M. Basset, S. Cadars, A. Lesage, C. Copéret, L. Emsley, *J. Am. Chem. Soc.* **2006**, *128*, 13545–13552; e) H. Zhang, H. Sun, E. Oldfield, *J. Am. Chem. Soc.* **2005**, *127*, 3652–3653; f) C. P. Grey, N. Dupré, *Chem. Rev.* **2004**, *104*, 4493–4512; g) H. Heise, F. H. Köhler, M. Herker, W. Hiller, *J. Am. Chem. Soc.* **2002**, *124*, 10823–10832; h) H. Heise, F. H. Köhler, F. Mota, J. J. Novoa, J. Veciana, *J. Am. Chem. Soc.* **1999**, *121*, 9659–9667.

[12] F. H. Köhler, R. Lescouëzec, *Angew. Chem.* **2004**, *116*, 2625–2627; *Angew. Chem. Int. Ed.* **2004**, *43*, 2571–2573.

[13] Recent examples : a) M. Schwarten, D. Babel, *Z. Anorg. Allg. Chem.* **2000**, *626*, 1921–1928; b) P. Franz, C. Ambrus, A. Hauser, D. Chernyshov, M. Hostettler, J. Hauser, L. Keller, K. Krämer, H. Stoeckli-Evans, P. Pattison, H.-B. Bürgi, S. Decurtins, *J. Am. Chem. Soc.* **2004**, *126*, 16472–16477, and references therein.

[14] a) A. Ludi, H. U. Güdel, *Helv. Chim. Acta* **1968**, *51*, 2006–2016; b) G. W. Beall, W. O. Milligan, J. Korp, I. Bernal, *Inorg. Chem.* **1977**, *16*, 2715–2718.

[15] a) B. Ziegler, M. Witzel, M. Schwarten, D. Babel, *Z. Naturforsch. B* **1999**, *54*, 870–876; b) J. Balmaseda, E. Reguera, A. Gomez, B. Diaz, M. Autie, *Microporous Mesoporous Mater.* **2002**, *54*, 285–292.

[16] Seven different cadmium sites are expected in principle, but statistical calculation based on the binomial law shows that only six signals could be observed, as the $Cd^{II}(OH_2\square)_6$ surrounding has a very low probability of existence (see the Supporting Information).

[17] P. G. Mennitt, M. P. Shatlock, V. J. Bartuska, G. E. Maciel, *J. Phys. Chem.* **1981**, *85*, 2087–2091.

[18] The composition of **1**–**5** was checked by elemental analysis and electron dispersion-activated X-ray spectroscopy (EDAX). The powder X-ray diffraction patterns of the samples (Figure SI1 in the Supporting Information) were typical for the cubic Prussian blue structure (see the Supporting Information).

[19] F. H. Köhler in *Magnetism: Molecules to Materials* (Eds.: J. S. Miller, M. Drillon), Wiley-VCH, Weinheim, **2001**, pp. 379–430.

